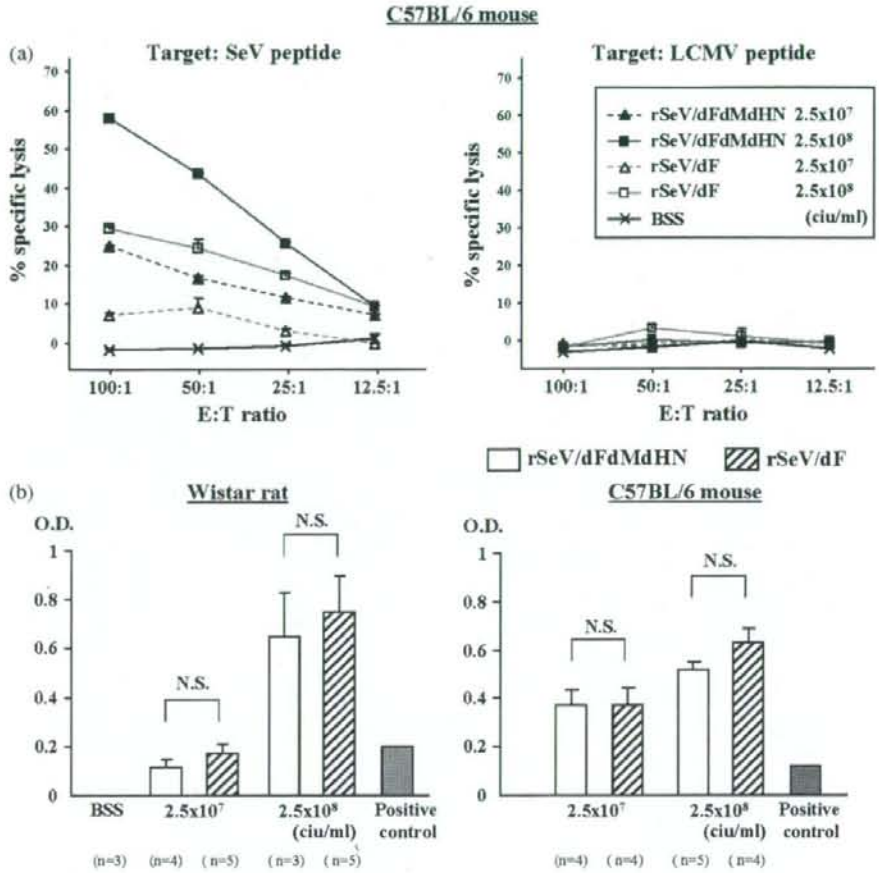

Figure 6. Assessment for SeV-specific adaptive immune response following subretinal injection of each rSeV. (a) The CTL activity of C57BL/6 mice treated with rSeV vectors was assessed with a standard ^{51}Cr-release assay. Ten days after subretinal injection, spleen cells were harvested from mice treated with rSeV/dF-EGFP (2.5×10^7 ciu/ml) (△), rSeV/dF-EGFP (2.5×10^8 ciu/ml) (□), rSeV/dFdMdHN-EGFP (2.5×10^7 ciu/ml) (▲), or rSeV/dFdMdHN-EGFP (2.5×10^8 ciu/ml) (■). Controls included BSS-injected mice (×). LCMV peptide was also used as a third-party (right panel). Note the stronger cell lysis activity in rSeV/dFdMdHN-treated mice at the same titer (left panel). The figure shows results from one of three similar experiments. (b) The production of anti-SeV antibodies 4 weeks after vector injection was assessed by ELISA. No significant difference could be found between the two types of vectors ($n = 3$–5 each)

of NP proteins. For further improvement of this vector system, we are now aiming to introduce mutations on the NP gene to modify the CTL response.

The duration of gene expression by rSeVs is transient in the present design; however, rSeV-mediated gene transfer has demonstrated efficient therapeutic effects in many animal models, including established tumor models. For example, the boost of IL-2 via intracerebral injection of rSeV resulted in a significant antitumor effect on brain tumors combining with peripheral vaccination [31]. In addition, we recently found that rSeV efficiently infects and activates dendritic cells, and the intratumor injection of rSeV-modified dendritic cells (DCs) has been shown to have a strong antitumor effect associated with enhanced CTL responses [32]. These rSeV-based cancer immunotherapies have demonstrated superior antitumor effects over the existing strategies. Thus, we are now assessing whether rSeV-based gene therapy could be an adjuvant therapy for bilateral retinoblastoma because its management is still difficult in some cases despite multimodal treatment approaches [2,33].

In conclusion, the present study showed that membranous gene-deleted rSeV retained efficient gene transfer and remarkably reduced the host innate immune response in ocular tissue. Moreover, vector-related retinal damage found using the previous SeV vector system was dramatically improved. These findings may extend the utility of this new vector system for retinal gene transfer, although the acquired immune response remains to be overcome for long-term transgene expression of rSeV. Therefore, further studies refining this vector system are required for the clinical availability of rSeV for ocular diseases.

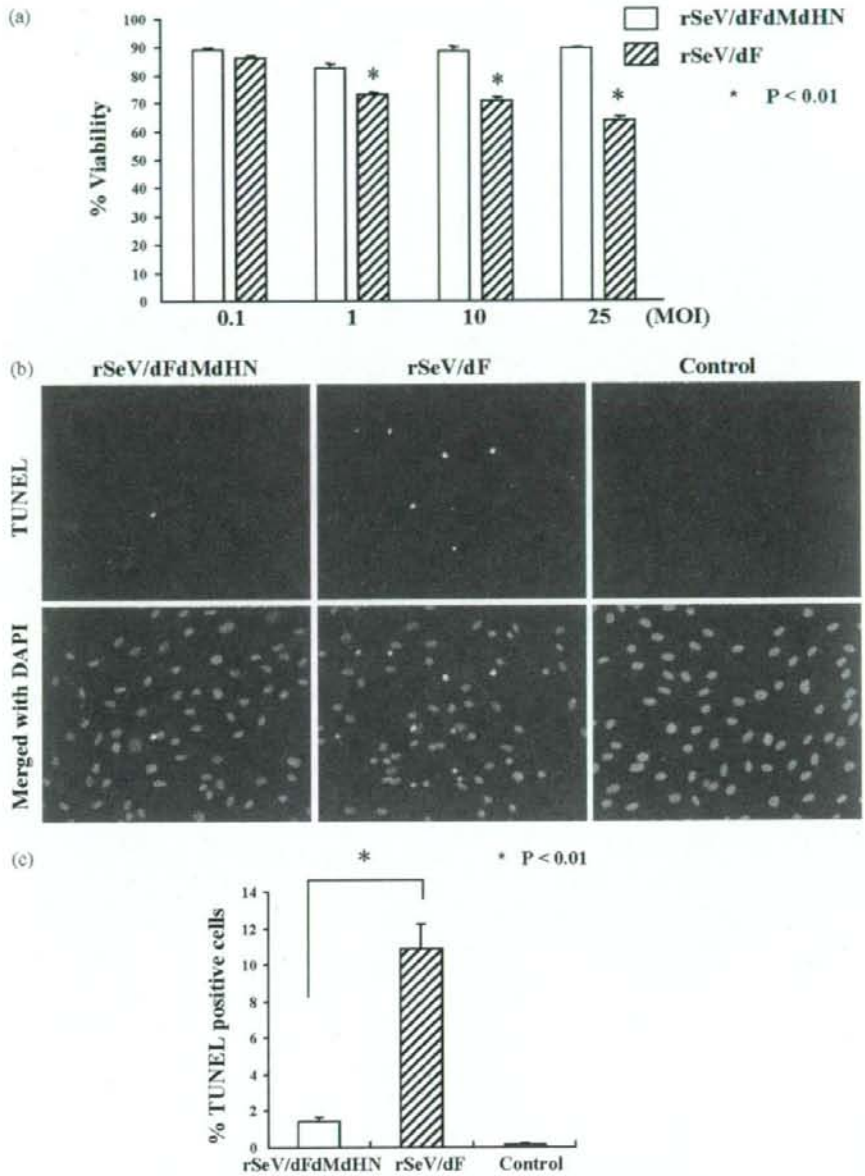

Figure 7. Quantitative analysis of rSeV infection-dependent cytotoxicity in vitro. (a) *In vitro* cytotoxicity of rSeVs to ARPE-19. After 48 h of culturing in the presence of rSeV/dF-EGFP or rSeV/dFdMdHN-EGFP at a multiplicity of infection (MOI) of 0.1, 1, 10 and 25, cell viability was assessed. Note the reduction of SeV-induced cytotoxicity in rSeV/dFdMdHN-infected cells ($n = 4$ each; $^*p < 0.01$). (b, c) TUNEL staining (b) and quantitative analysis of the TUNEL-positive apoptotic nuclei in ARPE-19 cells infected with each rSeV at a MOI of 10. Note the reduction of SeV-induced apoptosis in rSeV/dFdMdHN-infected cells ($n = 5$ each; $^*p < 0.01$)

Acknowledgements

We thank Drs Akihiro Tagawa, Takumi Kanaya, Hiroshi Ban and Takashi Hironaka for their excellent technical assistance in vector construction and large-scale production, and Mr Hiroshi Fujii and Miss Chie Arimatsu for assistance with the experiments. This work was supported in part by a Grant-in-Aid (to Y.I., Y.Y. and K.S.) from the Japanese Ministry of Education, Culture, Sports, Science and Technology. Dr Yonemitsu is a member of the Scientific Advisory Board of DNAVEC Corporation.

Supplementary Material

The supplementary electronic material for this paper is available in Wiley InterScience at: http://www.interscience.wiley.com/jpages/1099-498X/suppmat/.

References

1. Campochiaro PA, Nguyen QD, Shah SM, *et al.* Adenoviral vector-delivered pigment epithelium-derived factor for neovascular age-related macular degeneration: results of a phase I clinical trial. *Hum Gene Ther* 2006; **17**: 167–176.
2. Chevez-Barrios P, Chintagumpala M, Mieler W, *et al.* Response of retinoblastoma with vitreous tumor seeding to adenovirus-mediated delivery of thymidine kinase followed by ganciclovir. *J Clin Oncol* 2005; **23**: 7927–7935.
3. Bennett J. Commentary: an aye for eye gene therapy. *Hum Gene Ther* 2006; **17**: 177–179.
4. Lamb RA, Kolakofsky D. *Paramyxoviridae*: the viruses and their replication. In *Field's Virology*, Fields BN, Knipe DM, Howley PM (eds). Lippincott-Raven: Philadelphia, 1996; 1177–1204.
5. Nagai Y. Paramyxovirus replication and pathogenesis. Reverse genetics transforms understanding. *Rev Med Virol* 1999; **9**: 83–99.
6. Markwell MA, Svennerholm L, Paulson JC. Specific gangliosides function as host cell receptors for Sendai virus. *Proc Natl Acad Sci USA* 1981; **78**: 5406–5410.
7. Yonemitsu Y, Kitson C, Ferrari S, *et al.* Efficient gene transfer to airway epithelium using recombinant Sendai virus. *Nat Biotechnol* 2000; **18**: 970–973.
8. Masaki I, Yonemitsu Y, Komori K, *et al.* Recombinant Sendai virus-mediated gene transfer to vasculature: a new class of efficient gene transfer vector to the vascular system. *FASEB J* 2001; **15**: 1294–1296.
9. Moyer SA, Baker SC, Lessard JL. Tubulin: a factor necessary for the synthesis of both Sendai virus and vesicular stomatitis virus RNAs. *Proc Natl Acad Sci USA* 1986; **83**: 5405–5409.
10. Li HO, Zhu YF, Asakawa M, *et al.* A cytoplasmic RNA vector derived from nontransmissible Sendai virus with efficient gene transfer and expression. *J Virol* 2000; **74**: 6564–6569.
11. Ikeda Y, Yonemitsu Y, Sakamoto T, *et al.* Recombinant Sendai virus-mediated gene transfer into adult rat retinal tissue: efficient gene transfer by brief exposure. *Exp Eye Res* 2002; **75**: 39–48.
12. Yoshizaki M, Hironaka T, Iwasaki H, *et al.* Naked Sendai virus vector lacking all of the envelope-related genes: reduced cytopathogenicity and immunogenicity. *J Gene Med* 2006; **8**: 1151–1159.
13. Tanaka S, Yonemitsu Y, Yoshida K, *et al.* Impact of deletion of envelope-related genes of recombinant Sendai viruses on immune responses following pulmonary gene transfer of neonatal mice. *Gene Ther* 2007; **14**: 1017–1028.
14. Griffith TS, Brunner T, Fletcher SM, *et al.* Fas ligand-induced apoptosis as a mechanism of immune privilege. *Science* 1995; **270**: 1189–1192.
15. Streilein JW. Ocular immune privilege: therapeutic opportunities from an experiment of nature. *Nat Rev Immunol* 2003; **3**: 879–889.
16. Miyazaki M, Ikeda Y, Yonemitsu Y, *et al.* Simian lentiviral vector-mediated retinal gene transfer of pigment epithelium-derived factor protects retinal degeneration and electrical defect in Royal College of Surgeons rats. *Gene Ther* 2003; **10**: 1503–1511.
17. Ikeda Y, Goto Y, Yonemitsu Y, *et al.* Simian immunodeficiency virus-based lentivirus vector for retinal gene transfer: a preclinical safety study in adult rats. *Gene Ther* 2003; **10**: 1161–1169.
18. Shoji T, Yonemitsu Y, Komori K, *et al.* Intramuscular gene transfer of FGF-2 attenuates endothelial dysfunction and inhibits intimal hyperplasia of vein grafts in poor-runoff limbs of rabbit. *Am J Physiol Heart Circ Physiol* 2003; **285**: H173–H182.
19. Hua J, Liao MJ, Rashidbaigi A. Cytokines induced by Sendai virus in human peripheral blood leukocytes. *J Leukoc Biol* 1996; **60**: 125–128.
20. Mandelboim O, Lieberman N, Lev M, *et al.* Recognition of haemagglutinins on virus-infected cells by NKp46 activates lysis by human NK cells. *Nature* 2001; **409**: 1055–1060.
21. Arnon TI, Lev M, Katz G, *et al.* Recognition of viral hemagglutinins by NKp44 but not by NKp30. *Eur J Immunol* 2001; **31**: 2680–2689.
22. Bitzer M, Prinz F, Bauer M, *et al.* Sendai virus infection induces apoptosis through activation of caspase-8 (FLICE) and caspase-3 (CPP32). *J Virol* 1999; **73**: 702–708.
23. Holtkamp GM, Kijlstra A, Peek R, *et al.* Retinal pigment epithelium-immune system interactions: cytokine production and cytokine-induced changes. *Prog Retin Eye Res* 2001; **20**: 29–48.
24. Strauss O. The retinal pigment epithelium in visual function. *Physiol Rev* 2005; **85**: 845–881.
25. Kawai T, Akira S. Innate immune recognition of viral infection. *Nat Immunol* 2006; **7**: 131–137.
26. Bieback K, Lien E, Klagge IM, *et al.* Hemagglutinin protein of wild-type measles virus activates toll-like receptor 2 signaling. *J Virol* 2002; **76**: 8729–8736.
27. Kurt-Jones EA, Popova L, Kwinn L, *et al.* Pattern recognition receptors TLR4 and CD14 mediate response to respiratory syncytial virus. *Nat Immunol* 2000; **1**: 398–401.
28. Hou S, Doherty PC, Zijlstra M, *et al.* Delayed clearance of Sendai virus in mice lacking class I MHC-restricted CD8+ T cells. *J Immunol* 1992; **149**: 1319–1325.
29. Jiang LQ, Jorquera M, Streilein JW. Subretinal space and vitreous cavity as immunologically privileged sites for retinal allografts. *Invest Ophthalmol Vis Sci* 1993; **34**: 3347–3354.
30. Kast WM, Roux L, Curren J, *et al.* Protection against lethal Sendai virus infection by in vivo priming of virus-specific cytotoxic T lymphocytes with a free synthetic peptide. *Proc Natl Acad Sci USA* 1991; **88**: 2283–2287.
31. Iwadate Y, Inoue M, Saegusa T, *et al.* Recombinant Sendai virus vector induces complete remission of established brain tumors through efficient interleukin-2 gene transfer in vaccinated rats. *Clin Cancer Res* 2005; **11**: 3821–3827.
32. Shibata S, Okano S, Yonemitsu Y, *et al.* Induction of efficient antitumor immunity using dendritic cells activated by recombinant Sendai virus and its modulation by exogenous IFN-beta gene. *J Immunol* 2006; **177**: 3564–3576.
33. Shields CL, Meadows AT, Leahey AM, *et al.* Continuing challenges in the management of retinoblastoma with chemotherapy. *Retina* 2004; **24**: 849–862.

Guidelines for PDT in Japan

Dear Editor:

Guidelines for verteporfin therapy for choroidal neovascularization secondary to age-related macular degeneration (AMD) were published in 2002[1] and updated in 2005.[2] However, these guidelines were based on trials and clinical experience in predominantly Caucasian populations. The Japanese Age-Related Macular Degeneration Trial[3]—an open-label uncontrolled study—was designed to determine, in Japanese patients with evidence of classic subfoveal choroidal neovascularization due to AMD, whether verteporfin therapy had an effect and safety profile similar to those reported in predominantly Caucasian populations of the Treatment of AMD with Photodynamic Therapy Investigation.[4] A retrospective, open-label, multicenter, uncontrolled study was performed to provide additional efficacy and safety data on the use of verteporfin therapy for choroidal neovascularization secondary to AMD, in 471 eyes of 469 Japanese patients throughout 13 hospitals in Japan (Table 1 [all figures and tables available at http://aaojournal.org]). Subsequently, a roundtable discussion group of Japanese retina specialists was held on April 2, 2006 to develop guidelines for the use of verteporfin in Japan, based on interpretation of these data, which are summarized in this letter.

The study demonstrated that verteporfin was effective in maintaining visual acuity (VA) through 12 months for all lesion types (Fig 1, Table 2) as demonstrated previously in the Japanese Age-Related Macular Degeneration Trial.[3] Although verteporfin had positive effects on VA for lesions of all sizes, the greatest benefit was observed for eyes with small (≤1800-μm greatest linear dimension) lesions (Fig 2). Mean VA was maintained or improved for eyes with VA of 20/40 or worse at baseline; however, a decline was observed for eyes with good VA (>20/40; Fig 3). Visual acuity was maintained in older patients; however, verteporfin significantly ($P<0.001$) improved visual outcomes in patients younger than 60 (Fig 4). A significant improvement in VA was observed for eyes with polypoidal choroidal vasculopathy ($P<0.001$) (Fig 5), whereas the presence of hemorrhage or pigment epithelial detachment had no influence on VA.

Fluorescein leakage from choroidal neovascularization was stopped in approximately 65% of cases (Fig 6). Leakage was more likely to be absent in lesions with a smaller greatest linear dimension; however, the absence of leakage increased with time, regardless. Ocular adverse events were reported in only 45 (9.6%) treated eyes and systemic adverse events in 23 (4.9%) patients (Table 3). Patients received a mean of 2.0 treatments by month 12. The treatment frequency was lower for cases with polypoidal choroidal vasculopathy and higher for cases with hemorrhage; however, it was not influenced by lesion type or presence of pigment epithelial detachment through month 12 (Tables 4, 5).

The following recommendations are based on consensus opinion after discussion of the study data. The choroidal neovascularization location should be identified as subfoveal by fluorescein angiography or other methods, such as optical coherence tomography or indocyanine green angiography. At present, there is insufficient evidence to make recommendations about the use of verteporfin for extrafoveal or juxtafoveal choroidal neovascularization. The lesion composition can be predominantly classic, minimally classic, or occult with no classic choroidal neovascularization. Verteporfin is strongly recommended for lesions ≤1800 μm and eyes with larger lesions (< 5400 μm). Verteporfin should be considered for lesions > 5400 μm, although this must be balanced against an increased risk of VA deterioration. Verteporfin is recommended for eyes with baseline VA of 20/40 to 20/200 inclusive (Japanese Age-Related Macular Degeneration Trial criteria).[3] Verteporfin can be considered for cases with good (>20/40) VA, after discussion of the potential risks involved with the patient. A decrease in mean VA was observed for patients with VA>20/40 at baseline (n = 17); however, VA was improved or maintained for the majority of these patients. Verteporfin should also be considered for cases with low VA (<20/200) at baseline.

Age is not a consideration for use of verteporfin in Japanese patients. Although an improvement in VA was associated with younger age (<60 years), VA was maintained over 12 months for older patients. The presence of polypoidal choroidal vasculopathy was associated with improved outcomes after verteporfin therapy. The presence of hemorrhage or pigment epithelial detachment does not contraindicate the use of verteporfin.

An algorithm has been formulated to summarize the recommendations, which will be updated as new data become available (Fig 7).

YASUO TANO, MD
Osaka, Japan

ON BEHALF OF THE OPHTHALMIC PDT STUDY GROUP*

References

1. Verteporfin Roundtable 2000 and 2001 Participants, Treatment of Age-Related Macular Degeneration with Photodynamic Therapy (TAP) Study Group Principal Investigators, Verteporfin in Photodynamic Therapy (VIP) Study Group Principal Investigators. Guidelines for using verteporfin (Visudyne®) in photodynamic therapy to treat choroidal neovascularization due to age-related macular degeneration and other causes. Retina 2002;22:6–18.
2. Verteporfin Roundtable Participants. Guidelines for using verteporfin (Visudyne) in photodynamic therapy for choroidal neovascularization due to age-related macular degeneration and other causes: update. Retina 2005;25:119–34.
3. Japanese Age-Related Macular Degeneration Trial (JAT) Study Group. Japanese Age-Related Macular Degeneration Trial: 1-year results of photodynamic therapy with verteporfin in Japanese patients with subfoveal choroidal neovascularization secondary to age-related macular degeneration. Am J Ophthalmol 2003;136:1049–61.
4. Treatment of Age-Related Macular Degeneration with Photodynamic Therapy (TAP) Study Group. Photodynamic therapy of subfoveal choroidal neovascularization in age-related macular degeneration with verteporfin: one-year results of 2 randomized clinical trials—TAP report 1. Arch Ophthalmol 1999;117:1329–45.

*For Study Group members, see "Appendix" (available at http://aaojournal.org).

Table 1. Summary of Demographic and Baseline Characteristics

Characteristic	N (%)
Patients	469
Gender	
Women	159 (33.9)
Men	310 (66.1)
Age (yrs)	
40–49	3 (0.6)
50–59	38 (8.1)
60–69	128 (27.3)
70–79	212 (45.2)
80–89	84 (17.9)
≥90	4 (0.9)
Mean	72.0
Eyes	471
Decimal visual acuity (approximate Snellen equivalent)	
>0.5 (>20/40)	23 (4.9)
0.5–0.1 (20/40–20/200)	315 (66.9)
<0.1 (<20/200)	133 (28.2)
Mean	0.15
Median	0.15
Treated eye	
Right	232 (49.3)
Left	239 (50.7)
Location of lesion	
Subfoveal	458 (97.2)
Juxtafoveal	10 (2.1)
Extrafoveal	2 (0.4)
Cannot grade	1 (0.2)
Lesion type	
Predominantly classic	153 (32.5)
Minimally classic	140 (29.7)
Occult with no classic	178 (37.8)
Greatest linear dimension of lesion (μm)	
≤1800	49 (10.4)
>1800–3600	171 (36.3)
>3600–5400	184 (39.1)
>5400	67 (14.2)
Mean	3855.9
Median	3700.0
Polypoidal choroidal vasculopathy	
Yes	146 (31.0)
No	320 (67.9)
Unidentified	5 (1.1)
Hemorrhage	
Yes	334 (70.9)
No	136 (28.9)
Unidentified	1 (0.2)
Serous pigment epithelial detachment	
Yes	58 (12.3)
No	413 (87.7)

Appendix: Ophthalmic PDT Study Group

Yasuo Tano, Osaka University Medical School; Fumio Shiraga, Faculty of Medicine, Kagawa University; Kanji Takahashi, Kansai Medical University; Tatsuro Ishibashi, Kyushu University; Nagahisa Yoshimura, Graduate School of Medicine, Kyoto University; Shoji Kishi, Gunma University Graduate School of Medicine; Muneyasu Takeda, Sapporo City General Hospital; Shinobu Takeuchi, Toho University Ohashi Medical Center; Yuichiro Ogura, Nagoya City University Graduate School of Medical Sciences; Hiroko Terasaki, Nagoya University Graduate School of Medicine; Mitsuko Yuzawa, Surugadai Nihon University Hospital; Tomohiro Iida, Fukushima Medical University School of Medicine; Hiroyuki Iijima, Graduate School of Medicine and Engineering, Yamanashi University; Masahito Ohji, Shiga University Medical School; Annabelle A. Okada, Kyorin Eye Center, Kyorin University School of Medicine; Yasuhiro Tamaki, Graduate School of Medicine, University of Tokyo.

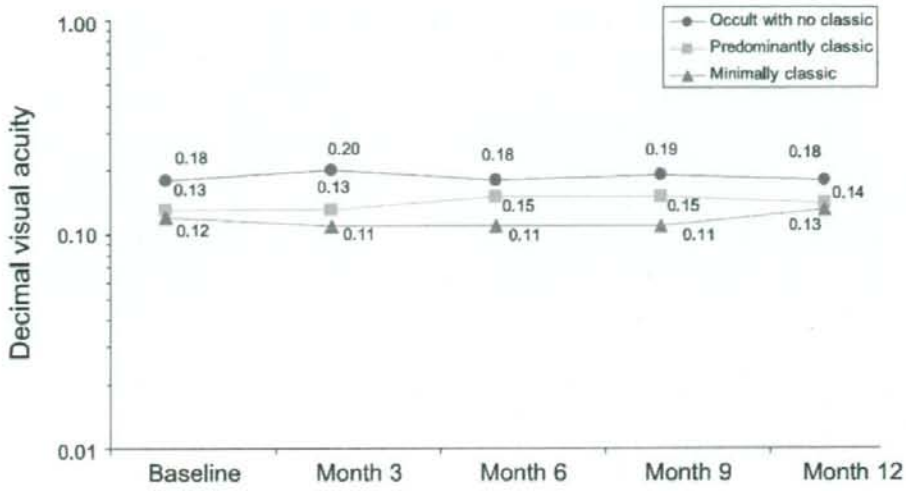

Figure 1. Mean visual acuity over time by lesion type.

Table 2. Decimal Visual Acuity (VA) for Study Eyes

	Baseline	Month 3	Month 6	Month 9	Month 12	P Value
Median	0.15	0.15	0.15	0.15	0.15	
Mean	0.15	0.15	0.15	0.15	0.15	0.597
Lesion type						
Predominantly classic	0.13	0.13	0.15	0.15	0.14	0.874
Minimally classic	0.12	0.11	0.11	0.12	0.13	0.210
Occult with no classic	0.18	0.20	0.18	0.19	0.18	0.760
Lesion size (GLD, μm)						
≤1800	0.18	0.21	0.26	0.24	0.29	<0.001
>1800–3600	0.17	0.17	0.17	0.17	0.17	0.923
>3600–5400	0.13	0.14	0.13	0.13	0.12	0.918
>5400	0.11	0.11	0.11	0.12	0.13	0.435
Baseline decimal VA (approximate Snellen equivalent)						
>0.5 (>20/40)	0.68	0.52	0.46	0.44	0.46	0.037
0.5–0.1 (20/40–20/200)	0.21	0.20	0.19	0.19	0.19	0.093
<0.1 (<20/200)	0.05	0.06	0.06	0.07	0.07	<0.001
Age (yrs)						
<60	0.14	0.19	0.23	0.24	0.24	<0.001
60–79	0.16	0.15	0.15	0.16	0.16	0.689
>80	0.10	0.11	0.10	0.10	0.09	0.751
PCV						
With	0.15	0.17	0.18	0.18	0.19	<0.001
Without	0.14	0.14	0.14	0.14	0.14	0.215
Hemorrhage						
With	0.14	0.14	0.14	0.14	0.14	0.969
Without	0.15	0.17	0.17	0.17	0.18	0.348
Serous pigment epithelial detachment						
With	0.15	0.18	0.15	0.15	0.15	0.476
Without	0.14	0.14	0.15	0.14	0.15	0.762

GLD = greatest linear dimension; PCV = polypoidal choroidal vasculopathy.
With the exception of median decimal VA, all values are for the mean decimal VA for study eyes.

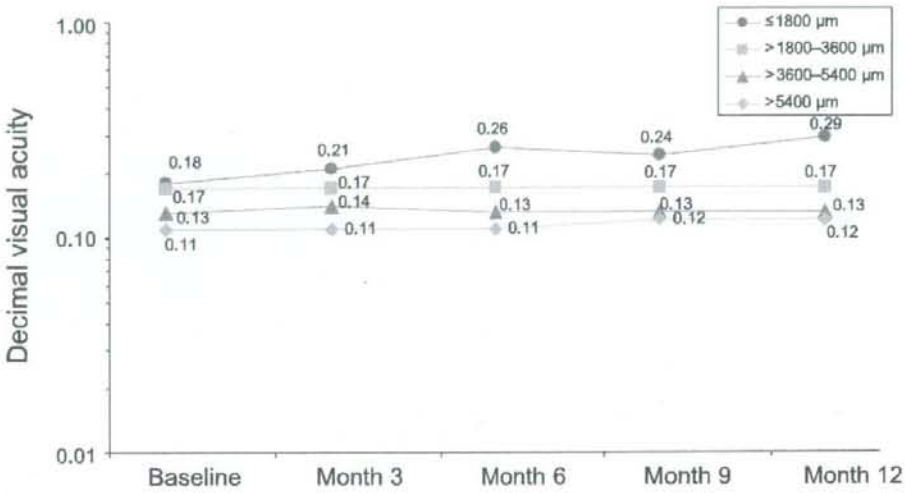

Figure 2. Mean visual acuity over time by lesion size.

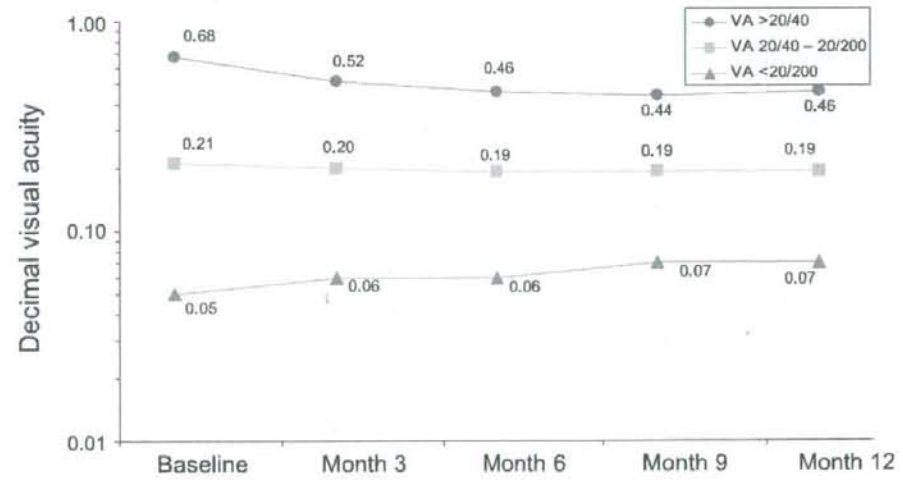

Figure 3. Mean visual acuity over time by baseline visual acuity (VA).

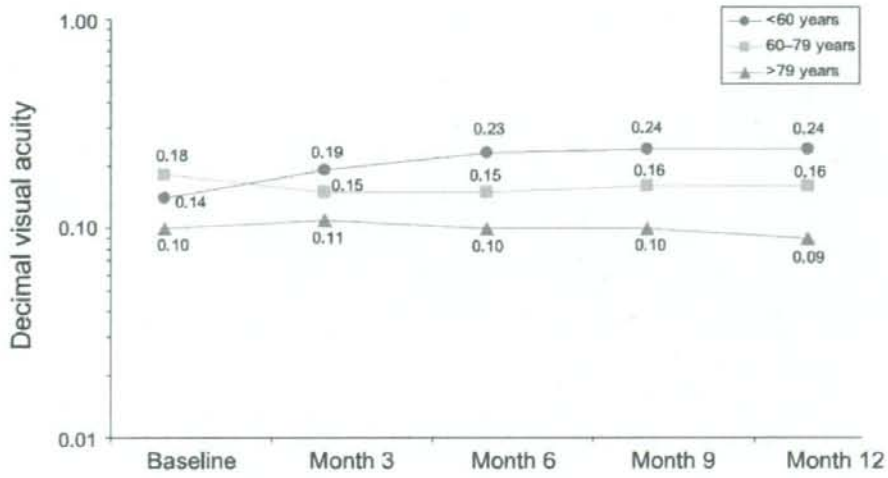

Figure 4. Mean visual acuity over time by patient age at baseline.

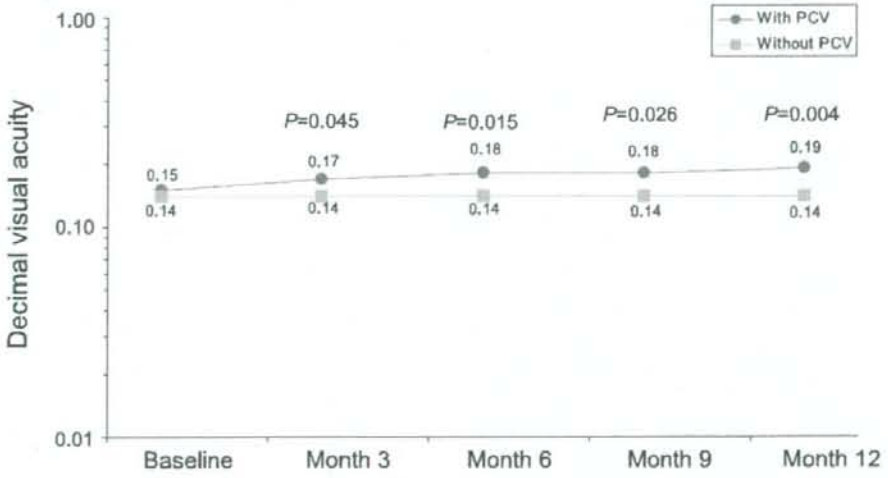

Figure 5. Mean visual acuity over time by presence or absence of polypoidal choroidal vasculopathy (PCV).

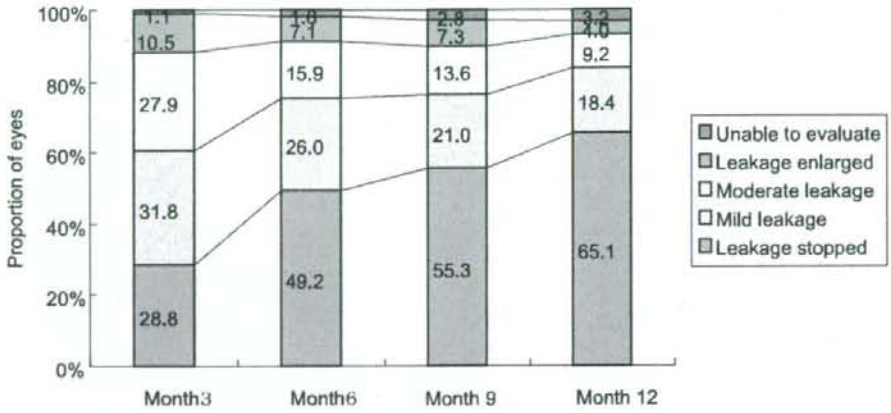

Figure 6. Angiographic outcomes: absence of fluorescein leakage from choroidal neovascularization at month 12.

Table 3. Incidence of Clinically Relevant Adverse Events

Event	No. of Patients or Eyes (%)
Ocular (total no. of eyes = 471)	
Total ocular events	45 (9.6)
Visual acuity deterioration	23 (4.9)
Subretinal hemorrhage	21 (4.5)
Retinal hemorrhage	7 (1.5)
Vitreous hemorrhage	6 (1.3)
Retinal detachment	3 (0.6)
Retinal pigment epithelial detachment	1 (0.2)
Others	5 (1.1)
Systemic (total no. of patients = 469)	
Total systemic events	23 (4.9)
Back pain	9 (1.9)
Headache	4 (0.9)
Others	13 (2.8)

Table 4. Patient Follow-up and Treatment Exposure through Month 12

Follow-up Visit	No. (%) of Patients Treated
Month 0	471 (100)
Month 3	218 (46)
Month 6	126 (27)
Month 9	84 (18)
Month 12	NA

NA = not applicable.
Mean = 1.91 treatments (2.00 treatments for the 428 eyes observed for 12 mos).

Table 5. Treatment Frequency through Month 12

Characteristic	Treatment Frequency	P Value
All eyes observed for 12 mos (n = 428)	2.00	
Lesion type		0.155
Predominantly classic	2.00	
Minimally classic	2.09	
Occult with no classic	1.92	
PCV		
With	1.88	0.043
Without	2.06	
Hemorrhage		
With	2.06	
<50%	2.07	
>50%	1.93	
Without	1.86	0.024
Serous pigment epithelial detachment		0.227
With	1.87	
Without	2.02	
Lesion size (GLD, μm)		0.279
≤1800	1.87	
>1800–3600	1.93	
>3600–5400	2.12	
>5400	1.95	
Baseline visual acuity		0.279
>20/40	1.75	
20/40–20/200	2.05	
<20/200	1.93	

GLD = greatest linear dimension; PCV = polypoidal choroidal vasculopathy.

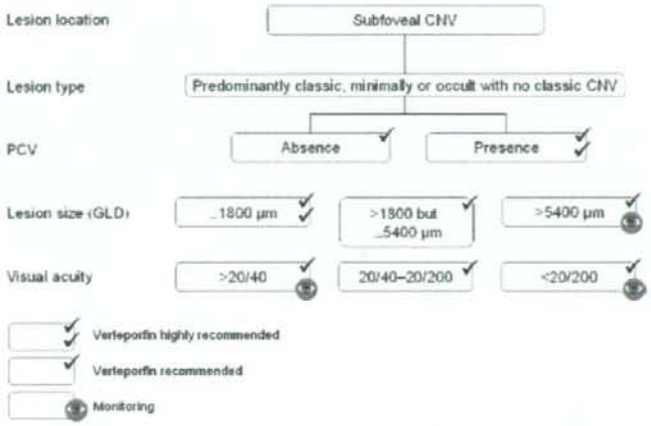

Figure 7. Algorithm summarizing the recommendations for the use of verteporfin in Japanese patients with choroidal neovascularization (CNV) secondary to age-related macular degeneration. GLD = greatest linear dimension; PCV = polypoidal choroidal vasculopathy.

BJO

The internal limiting membrane peeling with brilliant blue G staining for retinal detachment due to macular hole in high myopia

Y Mochizuki, H Enaida, T Hisatomi, Y Hata, M Miura, R Arita, S Kawahara, T Kita, A Ueno and T Ishibashi

Br. J. Ophthalmol. 2008;92;1009
doi:10.1136/bjo.2007.126300

LETTER

The internal limiting membrane peeling with brilliant blue G staining for retinal detachment due to macular hole in high myopia

Internal limiting membrane (ILM) peeling without dye is technically difficult in retinal detachment due to macular hole in high myopia (MHRD) with chorioretinal atrophy because of poor visualisation of ILM. Accordingly, a dye such as indocyanine green (ICG) or trypan blue (TB) is essential for facilitating ILM peeling. However, recent reports have emerged about retinal damage caused by ICG and TB both in experimental and clinical use.[1–4] There is a need to develop new dyes for effective and safe staining in order to facilitate ILM peeling. In the present study, we investigated the efficacy of a new dye: brilliant blue G (BBG) assisted ILM peeling for MHRDs.

CASE SERIES

This study was designed as a clinical case series. Six eyes of six patients with MHRD were recruited from the outpatient unit of Kyushu University Hospital, Japan. The possible advantages and risks of the present treatment were explained to the patients before surgery. Table 1 summarises the clinical characteristics of the six eyes included in this study. Triamcinolone acetonide (TA) solution was injected into the midvitreous cavity and a vitrectomy was performed. The white-coloured posterior vitreous cortex (VC) on the retinal surface was removed with ILM forceps and/or diamond-dusted membrane scraper. After this procedure, BBG solution with (concentration 0.25 mg/ml) was gently injected into the vitreous cavity to stain ILM and washed out immediately with balanced salt solution.[5] The light blue-coloured ILM was removed with ILM forceps. Subsequently, a fluid–air exchange was performed and followed by a gas or silicone oil in all cases. Postoperative examinations included slit-lamp microscopy, ophthalmoscopy, best corrected visual acuity (BCVA) and intraocular pressure. BBG dye selectively stained the ILM and allowed easier and safer removal of the ILM (fig 1). In all cases the retina remained attached. Complications such as retinal pigment epithelium atrophy related to BBG use were not identified in this study. The mean BCVA tended to improve from 1.32 (SD 0.38) (logMAR units 0.98 (SD 0.46)) after surgery, but there was no statistically significant difference. The postoperative follow up period ranged from 10 to 15 months with a mean follow up period of 12.3 (SD 1.9) months.

COMMENT

We used TA for identifying the posterior VC and could remove the posterior VC as previously reported.[6–8] As a result, BBG dye selectively stained the ILM and allowed easier and safer removal of the ILM. Recently ICG's and TB's safety has come into question.[1 9] Besides, TB did not provide sufficient staining of the ILM. We examined the morphological damage caused by subretinal injection of BBG, ICG or TB in a rat model. The results suggest that BBG would potentially show better biocompatibility and more safely in clinical applications than the previously reported dyes ICG and TB.[10] In MHRD, dyes could be dispersed and consequently introduced into the subretinal space through the macular hole. We therefore believe that the low potential toxicity and dying nature of BBG would make it more safe than ICG or TB. No other adverse effects due to BBG were observed within the observation period. We are now examining the safety and usefulness of BBG assisted membrane peeling for the long term as a clinical study.

Y Mochizuki, H Enaida, T Hisatomi, Y Hata, M Miura, R Arita, S Kawahara, T Kita, A Ueno, T Ishibashi

Departments of Ophthalmology, Graduate School of Medical Sciences, Kyushu University, Fukuoka, Japan

Correspondence to: Tatsuro Ishibashi, Department of Ophthalmology, Graduate School of Medical Sciences, Kyushu University, 3-1-1, Maidashi, Higashi-ku, Fukuoka, 812-8582, Japan; ishi@eye.med.kyushu-u.ac.jp

Funding: The study was supported in part by grants from the Ministry of Education, Science, Sports and Culture, Japan (Grant-in-Aid for Scientific Research #18791283).

Competing interests: None.

Ethics approval: The conduct of this study was approved by the institutional review board.

Table 1 Baseline clinical characteristics of six eyes

Case	Age (years)/ gender/eye	Visual acuity pre-op, post-op	Preoperative refraction (diopter)	Preoperative lens status	Optic axial length (mm)	Follow up (months)
1	70/M/R	20/100, 20/70	−13.5	Phakia	28.9	15
2	78/M/L	20/1000, 20/400	−4.75	Pseudophakia	28.4	14
3	64/F/R	20/300, 20/40	−4.25	Pseudophakia	27.4	12
4	69/M/L	20/200, 20/200	−18	Phakia	29.4	12
5	62/F/L	20/800, 20/200	−11.5	Phakia	28.1	11
6	81/F/R	20/1000, 20/1000	−13.5	Phakia	27.3	10

F, female; L, light; M, male; R, right.

Figure 1 Intraoperative view. After injection of brilliant blue G into vitreous cavity, internal limiting membrane (ILM) was clearly stained and grasped with ILM forceps. Arrows indicate the areas in which the ILM had already been removed. The areas can be clearly distinguished from areas of residual ILM.

Patient consent: Informed consent was obtained from all patients.

Br J Ophthalmol 2008;**92**:1009–1010.
doi:10.1136/bjo.2007.126300

REFERENCES

1. **Enaida H,** Sakamoto T, Hisatomi T, *et al.* Morphological and functional damage of the retina caused by intravitreous indocyanine green in rat eyes. *Graefes Arch Clin Exp Ophthalmol* 2002;**240**:209–13.
2. **Veckeneer M,** van Overdam K, Monzer J, *et al.* Ocular toxicity study of trypan blue injected into the vitreous cavity of rabbit eyes. *Graefes Arch Clin Exp Ophthalmol* 2001;**239**:698–704.
3. **Haritoglou C,** Gandorfer A, Gass CA, *et al.* Indocyanine green-assisted peeling of the internal limiting membrane in macular hole surgery affects visual outcome: a clinicopathologic correlation. *Am J Ophthalmol* 2002;**134**:836–41.
4. **Haritoglou C,** Gandorfer A, Schaumberger M, *et al.* Trypan blue in macular pucker surgery: an evaluation of histology and functional outcome. *Retina* 2004;**24**:582–90.
5. **Enaida H,** Hisatomi T, Hata Y, *et al.* Brilliant blue G selectively stains the internal limiting membrane/ brilliant blue G-assisted membrane peeling. *Retina* 2006;**26**:631–6.
6. **Sakaguchi H,** Ikuno Y, Choi JS, *et al.* Multiple components of epiretinal tissues detected by triamcinolone and indocyanine green in macular hole and retinal detachment as a result of high myopia. *Am J Ophthalmol* 2004;**138**:1079–81.
7. **Sakamoto T,** Miyazaki M, Hisatomi T, *et al.* Triamcinolone-assisted pars plana vitrectomy improves the surgical procedures and decreases the postoperative blood-ocular barrier breakdown. *Graefes Arch Clin Exp Ophthalmol* 2002;**240**:423–9.
8. **Mochizuki Y,** Hata Y, Enaida H, *et al.* Evaluating adjunctive surgical procedures during vitrectomy for diabetic macular edema. *Retina* 2006;**26**:143–8.
9. **Haritoglou C,** Gandorfer A, Schaumberger M, *et al.* Trypan blue in macular pucker surgery: an evaluation of histology and functional outcome. *Retina* 2004;**24**:582–90.
10. **Ueno A,** Hisatomi T, Enaida H, *et al.* Biocompatibility of brilliant blue G in a rat model of subretinal injection. *Retina* 2007;**27**:499–504.

Biochemical and Biophysical Research Communications 374 (2008) 38–43

Contents lists available at ScienceDirect

Biochemical and Biophysical Research Communications

journal homepage: www.elsevier.com/locate/ybbrc

Investigation of the role of CD1d-restricted invariant NKT cells in experimental choroidal neovascularization ☆

Kuniaki Hijioka [a], Koh-Hei Sonoda [a,*], Chikako Tsutsumi-Miyahara [a], Takeshi Fujimoto [a], Yuji Oshima [a], Masaru Taniguchi [b], Tatsuro Ishibashi [a]

[a] Department of Ophthalmology, Graduate School of Medical Sciences, Kyushu University, 3-1-1 Maidashi, Higashi-ku, Fukuoka 812-8582, Japan
[b] Laboratory for Immune Regulation, RIKEN Research Center for Allergy and Immunology, Suehiro-cho 1-7-22, Tsurumi, Yokohama, Kanagawa 230-0045, Japan

ARTICLE INFO

Article history:
Received 18 June 2008
Available online 9 July 2008

Keywords:
Choroidal neovascularization
Age-related macular degeneration
Natural killer T cell
Vascular endothelial growth factor
Innate immunity

ABSTRACT

Choroidal neovascularization (CNV) is directly related to visual loss in age-related macular degeneration and other macular disorders. We have investigated the role of CD1d-restricted invariant natural killer T (NKT) cells in laser-induced experimental CNV. Quantitative real-time PCR detected increased expression of NKT cell-related genes (*Vα14* and *CXCL16*) in whole eyes undergoing CNV, indicating local accumulation of NKT cells. We found a significant reduction of CNV and lower concentrations of vascular endothelial growth factor (VEGF) in ocular fluid in two different NKT cell-deficient mice, CD1d knockout (KO) and Jα18 KO mice. We also established *in vitro* co-cultures of retinal pigment epithelial cells and splenic NKT cells, and confirmed NKT cells could produce VEGF in the dish. Moreover, inoculating α-galactosylceramide, the ligand for NKT cells, into the vitreous cavity of C57BL/6 mice promoted CNV. We concluded that NKT cells play an important role in CNV as an inducer of VEGF.

Ocular neovascularization is responsible for the majority of cases of acquired blindness. There are two types of ocular neovascularization, which affect either the retina or the choroid. Retinal neovascularization is induced by hypoxia and occurs in diseases such as diabetic retinopathy and branch retinal vein occlusion. In contrast, choroidal neovascularization (CNV) results from abnormalities of Bruch's membrane and the retinal pigment epithelium (RPE) and is seen in patients with age-related macular degeneration (AMD), angioid streaks, high myopia, ocular histoplasmosis, and similar diseases. Most cases of CNV are induced by macular lesions, and it therefore directly causes severe loss of visual acuity in patients.

The exact cellular and molecular mechanisms that induce CNV remain to be elucidated. However, several recent reports demonstrated a role for the complement system, and particularly Factor H [1–3]. Patel et al. showed that elevated levels of autoantibodies against retinal antigens appeared in the sera of AMD patients [4]. In addition, we have shown a critical role for infiltrating macrophages and neutrophils in the eye, in the induction of experimental CNV [5]. Altogether, inflammatory process are clearly important in generating CNV.

NKT cells belong to a specialized population of lymphocytes that co-express the T cell receptor (TCR) αβ chains and NK markers [6] and are restricted by the MHC class I-like molecule, CD1d [7]. Since CD1d is also required for the development of NKT cells, CD1d knockout (KO) mice selectively lack these cells [8,9]. The majority of CD1d-restricted NKT cells are Vα14$^+$ and express a single invariant TCRα chain encoded by the Vα14Jα18 gene [7]. Jα18 KO mice have markedly reduced numbers of NKT cells in many organs [7]. Stimulated invariant NKT cells rapidly secrete large amounts of cytokines including IFN-γ and IL-4. Although the natural ligand which stimulates NKT cells remains to be identified, they have been reported to be stimulated by TCR ligation with the lipid antigen α-galactosylceramide (α-GalCer) presented by CD1d [10].

Our experimental goal was to confirm the role of invariant NKT cells in CNV and CNV-related diseases. Photocoagulation (PC)-induced CNV is a well-established animal model for investigating the mechanisms of human diseases [11]. We therefore induced experimental CNV in NKT-deficient mice and examined the cytokine profiles.

Materials and methods

Mice. Female 8- to 10-week-old mice were used in all experiments. C57BL/6 (B6) mice were obtained from SLC Japan (Shizuoka, Japan). CD1d KO mice were generated in the Transgenic Facility, Harvard Medical School (Boston, MA) and backcrossed to B6 mice for six generations. Jα18 KO mice (NKT KO mice) were generated

☆ *Grants:* This work was supported by grants from the Ministry of Education, Science, Sports and Culture, Japan (B1 No. 18390469: K.-H. Sonoda).

* Corresponding author. Fax: +81 92 642 5663.
E-mail address: sonodak@med.kyushu-u.ac.jp (K.-H. Sonoda).

0006-291X/$ - see front matter © 2008 Elsevier Inc. All right reserved.
doi:10.1016/j.bbrc.2008.06.080

at Chiba University (Chiba, Japan) and backcrossed eight times to B6 mice. All animals were housed in specific pathogen free conditions at Kyushu University. All animals were treated humanely and experiments conformed to the ARVO Statement for the Use of Animals in Ophthalmic and Vision Research.

Induction and evaluation of CNV. CNV was induced by photocoagulation (PC) and evaluated as previously described [5]. Briefly, laser photocoagulation (wave length 532 nm, 0.1 s, spot size 75 μm, power 200 mW) around the disc of the retina was administered to burn the posterior pole of the retina. A week later, mice were anesthetized and perfused with 1 ml phosphate buffered saline containing 50 mg/ml fluorescent-labeled dextran (25,000 MW; Sigma, St. Louis, MO) and the eyes were removed. The entire retina was mounted on slide glasses. The total area of hyperfluorescence associated with each burn, corresponding to the total number of fibrovascular scars, was measured using MacScope (version 2.3; Mitani, Fukui, Japan).

Real-time reverse transcriptase (RT)-PCR. Total RNA was extracted from whole eyes except for conjunctiva. Three eyes were pooled to obtain enough amount of mRNA for analysis, 12 or 24 h after PC using Trizol (Invitrogen Corp., Carlsbad, CA) according to the manufacturer's instructions. Aliquots containing 1 or 2 mg total RNA were reverse-transcribed using 1st Strand cDNA Synthesis Kit for RT-PCR (Roche Diagnostics, Indianapolis, IN) according to the manufacturer's instructions. The reverse-transcribed cDNAs were then subjected to real-time PCR using SYBR Premix Ex Taq (Takara Bio Inc., Otsu, Japan) and a Light Cycler (Roche Diagnostics GmbH, Mannheim, Germany). The primers used were 5′-CTAAGCACAGCACGCTGCA CA-3′ and 5′-AGGTATGACAATCAGCTGAGTCCC-3′ for *Vα14*, 5′-T CCTTTTCTTGTTGGCGCTG-3′ and 5′-CAGCGACACTGCCCTGGT-3′ for *CXCL16*, 5′-CCCTTTTGGGCCTATGCAG-3′ and 5′-ATGCCTCGAAG AGTTTTGCAC-3′ for *CXCR6*, 5′-TTACTGCTGTACCTCCACC-3′ and 5′-ACAGGACGGCTTGAAGATG-3′ for *VEGF*, 5′-TGGAGTCACAGAA GGAGTGGCTAAG-3′ and 5′-TCTGACCACAGTGAGGAATGTCC AC-3′ for *IL-6*, and 5′-GATGACCCAGATCATGTTTGA-3′ and 5′-GGAGA GCATAGCCCTCGTAG-3′ for β-actin. All estimated mRNA values were normalized to β-actin mRNA levels. Each experiment was repeated at least twice and representative data are shown.

Vitreous cavity injection. Low dose (500 ng/ml, 1 μl) or high dose (2.5 μg/ml, 1 μl) α-GalCer (Kirin Brewery Co. Ltd., Japan) or vehicle (500 ng/ml, 1 μl) was injected into the vitreous cavity using fine, 32-ga needles (Cat. No. 0160832, Hamilton, Reno, NV) and 10-μl syringes (Cat. No. 80330, Hamilton). The tip of the needles penetrated the sclera, choroid and retina, to reach the vitreous cavity and maximum volumes of 2 μl per injection were introduced per eye. We ensured that antigen was injected into the vitreous cavity by carefully guiding the tip of the needle under the microscope, through the flattened cornea covered by a glass microscope slide. Inoculating 2 μl solution elevated the intraocular pressure sufficiently to completely seal the retinal incision without any bleeding or detachment.

In vitro culture system. RPE cells were prepared from eyes of B6 mice and incubated for about 10 days in DMEM supplemented with 20% heat-inactivated fetal calf serum, 100 U/ml penicillin, 100 μg/ml streptomycin, 1% L-glutamine, and 0.1 mM non-essential amino acids at 37 °C in 5% CO_2. T lymphocytes from the spleens of B6 or CD1d KO mice were enriched on columns of IMMULAN goat anti-mouse IgG-coated beads (Biotex Laboratories, Houston, TX). RPE cells were plated in six-well dishes (Collagen-Coated Microplate 6 Well with Lid Collagen TypeI, IWAKI, Chiba, Japan) and incubated until almost confluent, and then the media was replaced to 2 ml of media containing about 2×10^6 T lymphocytes, and RPE cells and T lymphocytes were co-cultured with anti-CD1d antibody or control IgG for 6 h, when the culture supernatants were collected and used to measure cytokine and chemokine levels. Total RNA was also extracted from the floating T lymphocytes.

Luminex® assay. The concentrations of cytokines and chemokines were measured using a microbead-based ELISA system (Multiplex Ab Bead Kits; BioSource International, Camarillo, CA, USA) according to the manufacturer's directions with Luminex 100 (Luminex®, Austin, TX, USA). For *in vivo* experiments, eyes were enucleated from mice under deep anesthesia, conjunctival tissue was removed, and the remaining eye tissue was homogenized using a Biomasher (Nippi Inc., Tokyo, Japan). After centrifugation at 12,000*g* for 30 min, the supernatants were used in assays. For *in vitro* experiments, culture supernatants were used.

Statistics. Data were analyzed for significant differences between experimental groups using either ANOVA/Scheffe's test (more than three groups) or Student's *t*-test (two groups). *P* values $\leqslant 0.05$ were considered significant.

Results

Accumulation of NKT cells in the eye after laser treatment

First we measured the levels of invariant *Vα14* mRNA in the eye by using quantitative real-time PCR as previously reported [12]. Since Jiang et al. had reported that NKT cells are regulated by the chemokine *CXCL16* and its receptor *CXCR6*, which could be considered as new markers for NKT cells [13], we also measured local *CXCL16* expression. Total RNA was extracted from whole eyes of B6 mice, 24 h after laser treatment. *Vα14* and *CXCL16* mRNA were significantly elevated in eyes from laser-treated mice compared to untreated mice (Fig. 1), suggesting direct infiltration by invariant NKT cells in the eye in this model.

CNV in NKT cell-deficient mice

To determine whether the recruitment of NKT cells played a role in PC-induced CNV, we used two different NKT cell-deficient mice, and visualized the appearance of PC-induced CNV in choroidal flat mounts by fluorescent angiography. In contrast to wild-type mice, only a few hyperfluorescent areas of new vessel formation were observed in the KO mice, on day 7 after PC (Fig. 2A). The areas of CNV were shown to be statistically significantly smaller in the KO mice compared to wild-type mice (Fig. 2B). These observations suggested an important role for NKT cell infiltration in CNV development.

In vivo expression of angiogenic and/or inflammatory factors in NKT cell-deficient mice

Since NKT cells could mediate laser-induced angiogenesis, we reasoned that they probably synthesized or induced angiogenic and/or inflammatory factors. To identify candidate soluble factors that might be absent in NKT-deficient mice, we used microbead-based multi-protein analysis to compare B6 and CD1d KO mice after PC. Twelve hours after PC, ocular fluid samples from CD1d KO mice contained lower concentrations of angiogenic factors, such as VEGF and bFGF, than B6 mice, which was consistent with the reduced CNV in the KO mice. Interestingly, we found higher concentrations of IL-6 and keratinocyte-derived chemokine (KC), but lower concentrations of IL-12, IL-13, TNFα, IP-10, MIP-1α, and GM-CSF in CD1d KO than wild-type mice (data not shown). Among these soluble factors, we focused on VEGF and IL-6 expression. Consistent with the protein results, quantitative real-time PCR showed that mRNA expression was lower for *VEGF* and higher for *IL-6* in both NKT cell-deficient mice than in wild-type mice (Fig. 2C).

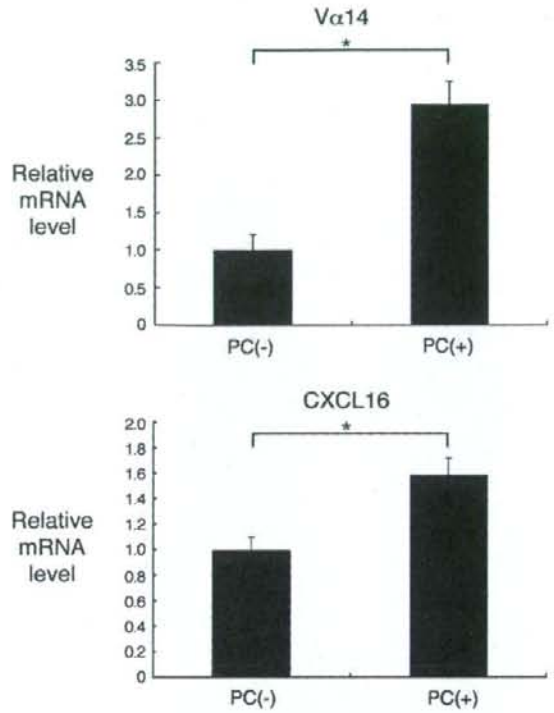

Fig. 1. Infiltration of NKT cells to the eye C57BL/6 mice were treated by laser and compared the expression of NKT cell marker (Vα14) and specific chemokine (CXCL16) with untreated mice. Twenty-four hours after laser, total RNA was extracted from the eyes and the amounts of *Vα14* and *CXCL16* mRNA were quantified by real-time RT-PCR and normalized by corresponding amounts of β-actin mRNA. Three eyes were pooled to obtain enough amount of mRNA ($n = 3$, total nine eyes were used). The bars show means ± SD. The experiments were repeated twice with similar results.

Effect of anti-CD1d antibody or the absence of NKT cells on the expression of VEGF and IL-6 in vitro

We next investigated *in vitro* expression of VEGF and IL-6 in co-cultures of RPE cells and column-enriched splenic T lymphocytes (Fig. 3A). The reason why we planned to use *in vitro* system was to investigate the cellular source of VEGF, since *in vivo* system had clear limitation f41or this purpose. We selected RPE as the stimulator of NKT cells, because RPE are major antigen-presenting cells in chorio-retinal interface that is damaged in AMD. When cells from B6 mice were cultured with anti-CD1d antibody, to inhibit NKT cell activity, culture supernatants collected after 6 h (Fig. 3) contained less VEGF than those from control IgG-treated cultures, at both the protein level, measured by ELISA, and at the mRNA level, measured in extracts of the floating T lymphocytes (Fig. 3B and C). In contrast, no difference was seen in IL-6 expression between anti-CD1d antibody-treated cultures and controls (Fig. 3B and C). Consistent results were seen when we used T cells from CD1d KO mice in cultures (Fig. 3D). Blocking of NKT-CD1d interaction by the specific antibody or the absence of NKT cells *in vitro* result in the decrease of VEGF, but not IL-6.

α-GalCer treatment promoted CNV and VEGF production in vivo

Since our results implicated NKT cells in CNV, we also looked at the effect of activating NKT cells on this process. α-GalCer is known to bind to NKT cells and induce various immune responses [10]. We therefore inoculated α-GalCer directly into the vitreous cavity and looked at the effect on CNV. As expected, α-GalCer inoculation increased CNV in B6 mice at low dose (100 ng/ml) compared to vehicle-treated mice (Fig. 4A). We also evaluated the effect of α-GalCer on the production of VEGF. Total mRNA was extracted from eyes of B6 mice 12 h after PC + α-GalCer injection into the vitreous cavity, and the amounts of *VEGF* mRNA was quantified by real-time RT-PCR. *VEGF* expression was higher in low dose α-GalCer-treated mice than vehicle-treated mice (Fig. 4B).

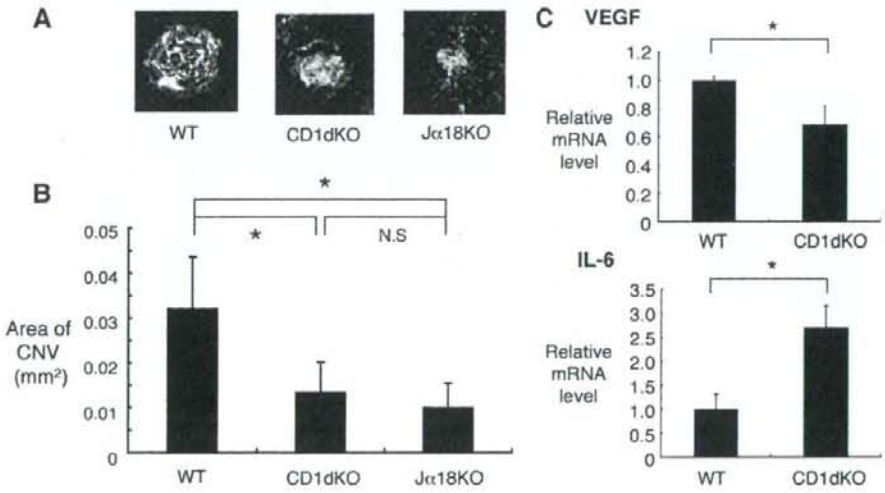

Fig. 2. CNV in NKT cell-deficient mice. C57BL/6 mice (WT), CD1d KO mice and Jα18 KO mice were treated by laser. The areas of CNV were compared between the three groups. The each experiments were repeated at least three times with similar results. (A) The representative CNV lesions of choroidal flat mount. Seven days after PC, the mice were perfused with fluorescein labeled dextran and choroidal flat mounts were made. CNV was detected as a hyperfluorescence vascular structure. (B) The area of CNV was compared among the three groups. The bars show means ± SD, $n = 8$. (C) Twelve hours after PC, total RNA was extracted and the amounts of *VEGF* (upper panel) and *IL-6* mRNA (lower panel) was quantified by real-time RT-PCR and normalized by corresponding amounts of β-actin mRNA. The bars show means ± SD, $n = 3$.

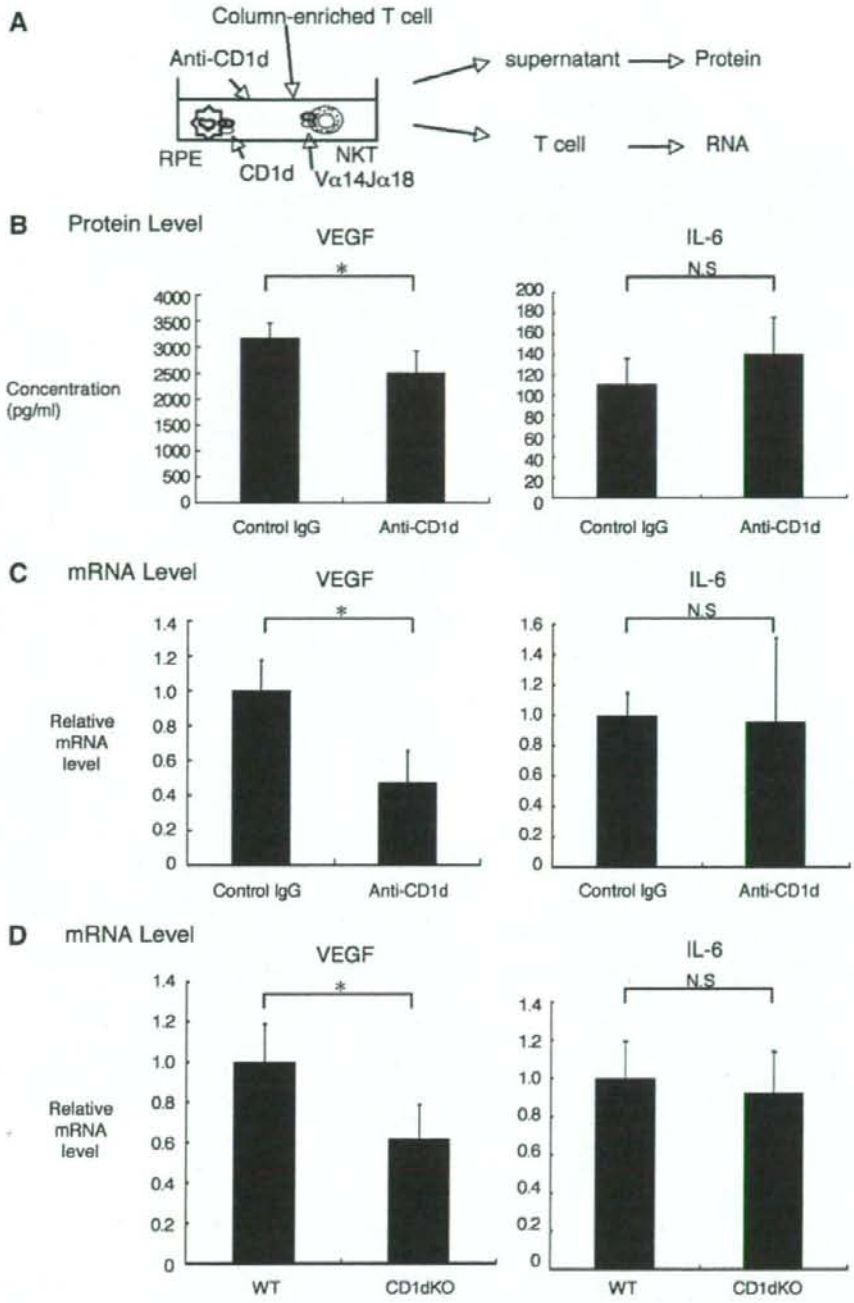

Fig. 3. *In vitro* expression of *VEGF* and *IL-6* from (adherent) T cells under treatment of anti-CD1d antibody. The each experiments were repeated more than twice with similar results. (A) RPE were prepared from eyes of C57BL/6 mice and incubated for about 10 days. After that, (adherent) RPE cells and (non-adherent) T lymphocytes, which were enriched from splenocytes of either C57BL/6 mice were co-cultured with anti-CD1d antibody or control IgG for 6 h. And then the culture supernatant was subjected to ELISA, and total RNA was extracted from floating T lymphocytes. Some experiments used splenic T cells from CD1d KO mice instead of using anti-CD1d antibody. (B) Culture supernatant was subjected to ELISA, and the concentration of VEGF and IL-6 was compared between two groups. The bars show means ± SD (triplicate wells). (C) Total RNA was extracted from floating T lymphocytes and the amounts of *VEGF* and *IL-6* mRNA was quantified by real-time RT-PCR and normalized by corresponding amounts of β-actin mRNA. The bars show means ± SD. Data represent the mean of three different well of samples. (D) The experiment used splenic T cells from CD1d KO mice instead of using anti-CD1d antibody.

Although 100 ng/ml range of α-GalCer must be the physiological dose, we unexpectedly found that higher dose of α-GalCer (500 ng/ml) reduced CNV (Fig. 4A) and VEGF (Fig. 4B). In fact, the dose-dependent different manner of response against α-GalCer has reported [14]. Since NKT cells can regulate immune response in multiple ways, we speculated that "high dose" α-GalCer might

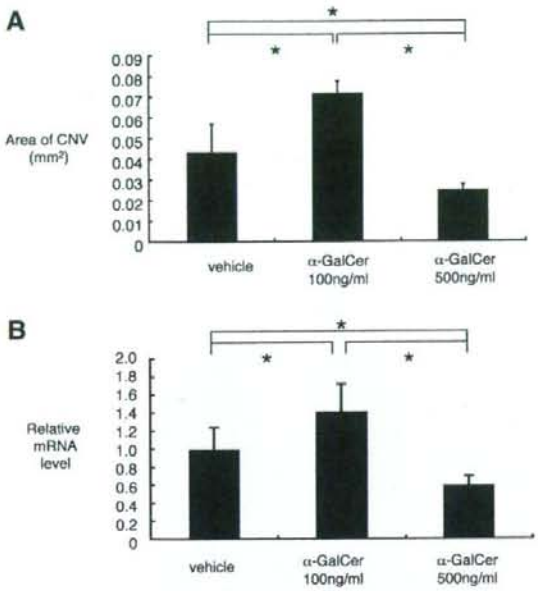

Fig. 4. *In vivo* α-GalCer treatment after laser. (A) C57BL/6 mice were treated by laser. Immediately after PC, 1 μl of vehicle (500 ng/ml) or α-GalCer (500 ng/ml or 2.5 mg/ml) was injected into vitreous cavity. Since the volume of vitreous fluid in mice is approximately 5 ml, the adjacent concentration of α-GalCer was around 100 ng/ml and 500 ng/ml, respectively. Seven days later, the mice were perfused with fluorescein labeled dextran and the eyes were removed to make choroidal flat mounts. CNV was detected as a hyperfluorescence vascular structure. The area of CNV was measured as described in Materials and methods. The bars show means ± SD, $n = 4$. The experiments were repeated at least three times with similar results. (B) Immediately after PC, 1 μl of vehicle or α-GalCer was injected into vitreous cavity. Twelve hours later, mice were sacrificed and their eyes were enucleated, and then eyes were homogenized and centrifuged. Total RNA was extracted from eyes (per three eyes) and the amounts of *VEGF* mRNA was quantified by real-time RT-PCR and normalized by corresponding amounts of β-actin mRNA. The bars show means ± SD. Data represent the mean of three independent sets of samples. The experiments were repeated twice with similar results.

activate NKT cells differently to produce some angiostatic factors and so may have therapeutic potential *in vivo*.

Discussion

Our data demonstrated for the first time that CD1d-restricted NKT cells play an important role in the formation of PC-induced CNV. After the type of insult reproduced by laser burns, NKT cells migrate to the eye and modulate the resulting inflammatory process associated with CNV.

Although NKT cells can directly produce VEGF *in vitro* (Fig. 3), it does not exclude possibility that other cells than NKT cells can also produce VEGF or somehow participate in CNV formation. In CNV, several reports have demonstrated RPE cells, microglia and infiltrating bone marrow-derived macrophages as sources of VEGF [15,16]. We currently postulate that NKT cells might also augment the production of VEGF by other cells in the eye rather than produce angiogenic factors themselves. In fact, NKT cells have been shown to activate macrophages either through a direct cell-to-cell or a cytokine mediated process [17].

We need to discuss about the diversity of effect that intravitreous α-GalCer can have on NKT cells. Its effect may depend upon the conditions, such as the dose and/or timing of inoculations [16]. Our data shows α-GalCer treatment *in vivo* enhanced CNV at "low dose" but reduced at "high dose". Since 100 ng/ml range of α-GalCer is the physiological dose, we speculate "high dose" α-GalCer may activate NKT cells differently to produce angiostatic factors. Our data also suggests that inoculating "high dose" α-GalCer into the vitreous cavity can have therapeutic potential. Controlled studies to evaluate the effects of different doses and times of administration of α-GalCer into the vitreous cavity will be needed to investigate its therapeutic use in CNV-related, sight-threatening diseases.

Although we found that NKT cell-deficient mice expressed low levels of the angiogenic factor VEGF, we found high levels of IL-6 expression compared to wild-type mice. Contradictory, several reports have shown that IL-6 promotes angiogenesis by inducing VEGF expression [18,19]. The mechanisms involved here are unclear, but Hatzi et al. have reported that IL-6 inhibited VEGF-induced corneal neovascularization [20]. Since IL-6 is known to be a multifunctional cytokine, it may have anti-angiogenic functions under some circumstances or at certain stages of inflammation. Another explanation is that NKT cells may promote VEGF induction by IL-6, and that the IL-6 overproduction in NKT cell-deficient mice was a response to the lower expression of VEGF in these mice. However, it is important to note that IL-6 concentrations were not raised in the co-cultures of RPE and NKT cells (Fig. 3). We speculate that the cellular source of IL-6 may be missing in this system, neither RPE nor NKT cells being the source, and we suggest that microglia and/or infiltrating macrophages in the eye may produce IL-6 *in vivo*. Further studies will be required to elucidate these mechanisms.

In summary, CD1d-restricted NKT cells, a type of innate immune cell, play an important role in PC-induced CNV. The therapeutic potential of modulating NKT cell activity with higher dose α-GalCer in sight-threatening eye disease warrants further research in this area.

Acknowledgment

We thank Ms. Michiyo Takahara for technical support.

References

[1] R.J. Klein, C. Zeiss, E.Y. Chew, J.Y. Tsai, R.S. Sackler, C. Haynes, A.K. Henning, J.P. SanGiovanni, S.M. Mane, S.T. Mayne, M.B. Bracken, F.L. Ferris, J. Ott, C. Barnstable, J. Hoh, Complement factor H polymorphism in age-related macular degeneration, Science 308 (2005) 385–389.
[2] A.O. Edwards, R. Ritter 3rd., K.J. Abel, A. Manning, C. Panhuysen, L.A. Ferrer, Complement factor H polymorphism and age-related macular degeneration, Science 308 (2005) 421–424.
[3] J.L. Haines, M.A. Hauser, S. Schmidt, W.K. Scott, L.M. Olson, P. Gallins, K.L. Spencer, S.Y. Kwan, M. Noureddine, J.R. Gilbert, N. Schnetz-Boutaud, A. Agarwal, E.A. Postel, M.A. Pericak-Vence, Complement factor H variant increases the risk of age-related macular degeneration, Science 308 (2005) 419–421.
[4] N. Patel, M. Ohbayashi, A.K. Nugent, K. Ramcha, M. Toda, K.Y. Chau, C. Bunce, A. Webster, A.C. Bird, S.J. Ono, V. Chong, Circulating anti-retinal antibodies as immune markers in age-related macular degeneration, Immunology 115 (2005) 422–430.
[5] C. Tsutsumi-Miyahara, K.H. Sonoda, K. Egashira, M. Ishibashi, H. Qiao, T. Oshima, T. Murata, M. Miyazaki, I.F. Charo, S. Hamano, T. Ishibashi, The relative contributions of each subset of ocular infiltrated cells in experimental choroidal neovascularization, Br. J. Ophthalmol. 88 (2004) 1217–1222.
[6] A. Bendelac, O. Lantz, M.E. Quimby, J.W. Yewdell, J.R. Bennink, R.R. Brutkiewicz, CD1 recognition by mouse NK1⁺ T lymphocytes, Science 268 (1995) 863–865.
[7] M. Taniguchi, M. Harada, S. Kojo, T. Nakayama, H. Wakao, The regulatory role of Valpha14NKT cells in innate and acquired immune response, Annu. Rev. Immunol. 21 (2003) 483–513.
[8] Y.H. Chen, N.M. Chiu, M. Mandal, N. Wang, C.R. Wang, Impaired NK1⁺ T cell development and early IL-4 production in CD1-Deficient mice, Immunity 6 (1997) 459–467.
[9] S.K. Mendiratta, W.D. Martin, S. Hong, A. Boesteanu, S. Joyce, L. Van Kaer, CD1d1 mutant mice are deficient in natural T cells that promptly produce IL-4, Immunity 6 (1997) 469–477.
[10] T. Kawano, J. Cui, Y. Koezuka, I. Toura, Y. Kaneko, K. Motoki, H. Ueno, R. Nakagawa, H. Sato, E. Kondo, H. Koseki, M. Taniguchi, CD1d-restricted and TCR-mediated activation of valpha14 NKT cells by glycosylceramides, Science 278 (1997) 1626–1629.
[11] E.T. Dobi, C.A. Puliafito, M. Destro, A new model of experimental choroidal neovascularization in the rat, Arch. Ophthalmol. 107 (1989) 264–269.
[12] M. Shimamura, T. Ohteki, U. Beutner, H.R. MacDonald, Lack of directed Vα14-Jα281 rearrangements in NK1⁺ T cells, Eur. J. Immunol. 27 (1997) 1576–1579.

[13] X. Jiang, T. Shimaoka, S. Kojo, M. Harada, H. Watarai, H. Wakao, N. Ohkohchi, S. Yonehara, M. Taniguchi, K. Seino, Critical role of CXCL16/CXCR6 in NKT cell trafficking in allograft tolerance, J. Immunol. 175 (2005) 2051–2055.
[14] M.T. Wilson, C. Johansson, D. Olivares-Villagomez, A.K. Singh, A.K. Stanic, C.R. Wang, S. Joyce, M.J. Wick, L. Van Kaer, The response of natural killer T cells to glycolipid antigens is characterized by surface receptor down-modulation and expansion, Proc. Natl. Acad. Sci. USA 100 (2003) 10913–10918.
[15] T. Ishibashi, Y. Hata, H. Yoshikawa, K. Nakagawa, K. Sueishi, H. Inomata, Expression of vascular endothelial growth factor in experimental choroidal neovascularization, Grafes. Arch. Clin. Exp. Ophthalmol. 235 (1997) 159–167.
[16] X. Yi, N. Ogata, M. Komada, C. Yamamoto, K. Takahashi, K. Omori, M. Uyama, Vascular endothelial growth factor expression in choroidal neovascularization in rats, Grafes. Arch. Clin. Exp. Ophthalmol. 235 (1997) 313–319.
[17] E.E. Nieuwenhuis, T. Matsumoto, M. Exley, R.A. Schleipman, J. Glickman, D.T. Bailey, N. Corazza, S.P. Colgan, A.B. Onderdonk, R.S. Blumberg, CD1d-dependent macrophage-mediated clearance of pseudomonas aeruginosa from lung, Nat. Med. 8 (2002) 588–593.
[18] T. Cohen, D. Nahari, L.W. Cerem, G. Neufeld, B.Z. Levi, Interleukin 6 induces the expression of vascular endothelial growth factor, J. Biol. Chem. 271 (1996) 736–741.
[19] S.P. Huang, M.S. Wu, C.T. Shun, H.P. Wang, M.T. Lin, M.L. Kuo, J.T. Lin, Interleukin-6 increases vascular endothelial growth factor and angiogenesis in gastric carcinoma, J. Biomed. Sci. 11 (2004) 517–527.
[20] E. Hatzi, C. Murphy, A. Zoephel, H. Rasmussen, L. Morbidelli, H. Ahorn, K. Kunisada, U. Tontsch, M. Klenk, K. Yamauchi-Takihara, M. Ziche, E.K. Rofstad, L. Schweigerer, T. Fotsis, N-myc oncogene overexpression down-regulates IL-6; evidence that inhibits angiogenesis and suppresses neuroblastoma tumor growth, Oncogene 21 (2002) 3552–3561.

Potent Inhibition of Cicatricial Contraction in Proliferative Vitreoretinal Diseases by Statins

Shuhei Kawahara,[1] Yasuaki Hata,[1] Takeshi Kita,[1] Ryoichi Arita,[1] Muneki Miura,[1] Shintaro Nakao,[2] Yasutaka Mochizuki,[1] Hiroshi Enaida,[1] Tadahisa Kagimoto,[3] Yoshinobu Goto,[4] Ali Hafezi-Moghadam,[2] and Tatsuro Ishibashi[1]

OBJECTIVE—Despite tremendous progress in vitreoretinal surgery, certain postsurgical complications limit the success in the treatment of proliferative vitreoretinal diseases (PVDs), such as proliferative diabetic retinopathy (PDR) and proliferative vitreoretinopathy (PVR). One of the most significant complications is the cicatricial contraction of proliferative membranes, resulting in tractional retinal detachment and severe vision loss. Novel pharmaceutical approaches are thus urgently needed for the management of these vision-threatening diseases. In the current study, we investigated the inhibitory effects of statins on the progression of PVDs.

RESEARCH DESIGN AND METHODS—Human vitreous concentrations of transforming growth factor-β2 (TGF-β2) were measured by enzyme-linked immunosorbent assay. TGF-β2– and vitreous-dependent phosphorylation of myosin light chain (MLC), a downstream mediator of Rho-kinase pathway, and collagen gel contraction simulating cicatrical contraction were analyzed using cultured hyalocytes. Inhibitory effects of simvastatin on cicatrical contraction were assessed both in vitro and in vivo.

RESULTS—Human vitreous concentrations of TGF-β2 were significantly higher in the samples from patients with PVD compared with those without PVD. Simvastatin inhibited TGF-β2–dependent MLC phosphorylation and gel contraction in a dose- and time-dependent manner and was capable of inhibiting translocation of Rho protein to the plasma membrane in the presence of TGF-β2. Vitreous samples from patients with PVD enhanced MLC phosphorylation and gel contraction, whereas simvastatin almost completely inhibited these phenomena. Finally, intravitreal injection of simvastatin dose-dependently prevented the progression of diseased states in an in vivo model of PVR.

CONCLUSIONS—Statins might have therapeutic potential in the prevention of PVDs. ***Diabetes* 57:2784–2793, 2008**

From the [1]Department of Ophthalmology, Graduate School of Medical Sciences, Kyushu University, Maidashi, Higashi-Ku, Fukuoka, Japan; the [2]Massachusetts Eye and Ear Infirmary, Department of Ophthalmology, Harvard Medical School, Boston, Massachusetts; [3]Aqumen Biopharmaceuticals, Tenjin, Chuo-Ku, Fukuoka, Japan; and the [4]Department of Occupational Therapy, Faculty of Rehabilitation, International University of Health and Welfare at Okawa, Enokizu, Okawa, Fukuoka, Japan.

Corresponding author: Yasuaki Hata, hatachan@med.kyushu-u.ac.jp.

Received 2 March 2007 and accepted 26 June 2008.

Published ahead of print at http://diabetes.diabetesjournals.org on 3 July 2008. DOI: 10.2337/db08-0302.

Proliferative vitreoretinal diseases (PVDs), such as proliferative diabetic retinopathy (PDR) and proliferative vitreoretinopathy (PVR), are common causes of severe vision loss (1). Surgical approaches for the treatment of these diseases have evolved significantly in the recent past, but the occurrence of postoperative complications, such as cicatricial contraction, limit the therapeutic success (2). Therefore, there is an urgent need for alternate pharmacological treatments of PVDs that can complement or potentially replace surgical intervention. In PDR and PVR, excessive wound healing and fibrosis induce the formation of proliferative membranes on the retinal surface. The proliferative membrane then extends into the vitreous and contracts, causing tractional detachment (3). The proliferative membrane consists of various cells, including hyalocytes, retinal pigment epithelial cells, glial cells, and fibroblast-like cells (4–7).

Hyalocytes morphologically resemble macrophages and are considered to originate from peripheral blood monocytes (8). Under physiological conditions, hyalocytes are mainly located in the cortical vitreous and are considered to maintain its transparency (9,10). Under pathological conditions, hyalocytes are thought to be critical in vitreoretinal interface diseases, such as idiopathic epiretinal membrane formation, macular hole, and diabetic macular edema (11). Hyalocytes in diabetic eyes are higher in number and of different shape compared with those in normal eyes (12).

Transforming growth factor-β (TGF-β) is pivotal to tissue fibrosis. Among the three isoforms of TGF-β, TGF-β2 is the predominant isoform in the vitreous (13,14). We and others have shown that TGF-β2 is overexpressed in the epiretinal membrane and vitreous of PDR and PVR patients and that its expression correlates with the presence of intraocular fibrosis (14–17). TGF-β2 modulates the differentiation of various cell types and is considered to increase the production of extracellular matrix, resulting in the formation and contraction of proliferative membranes (18,19). Thus, it is possible that the combination of hyalocytes and TGF-β2 may contribute to the pathogenesis of PVDs.

Statins, inhibitors of the 3-hydroxy-3-methyl-glutaryl (HMG)-CoA reductase, are widely used to reduce endogenous cholesterol synthesis and improve hypercholesterolemia (20). HMG-CoA reductase is an upstream enzyme in the mevalonate biosynthetic pathway that catalyzes the conversion of HMG-CoA into mevalonate and then, in a number of steps, into farnesylpyrophosphate (FPP), a precursor of cholesterol (21). By inhibiting HMG-CoA reductase, statins block the mevalonate pathway, resulting

in reduced synthesis of FFP and cholesterol. Statins are divided into three categories: the natural (i.e., lovastatin and pravastatin), the semisynthetic (i.e., simvastatin), and the synthetic (i.e., atorvastatin, fluvastatin, and cerivastatin). Statins decrease the risk for cardiovascular events even among high-risk individuals with coronary disease and diabetes (22). Moreover, statins may be useful in the treatment of other conditions, such as osteoporosis (23) and cancer growth and metastasis (24,25).

Another product of the mevalonate pathway is geranylgeranylpyrophosphate (GGPP), which is synthesized from FPP. Both FPP and GGPP are important isoprenoid intermediates and serve as lipid attachments for a variety of intracellular proteins to the plasma membrane, including the γ-subunit of heterotrimeric G-proteins and the small GTP-binding proteins, such as Ras and Rho, resulting in their activation (26). Rho translocation from the cytoplasm to the plasma membrane is dependent on geranylgeranylation (GGPP attachment), whereas Ras translocation is dependent on farnesylation (FPP attachment) (27). Rho in the plasma membrane is implicated in the cytoskeletal responses to extracellular signals and is converted to an active GDP-bound state (28). Rho-kinase, one of the effector molecules of Rho, is involved in a variety of cellular events related to cell morphology, adhesion, and motility (28–30), especially through phosphorylation of the myosin light chain (MLC). MLC phosphorylation induces actin-myosin interaction and, consequently, smooth muscle contraction and stress fiber formation in nonmuscle cells (31,32). Activation of the Rho/Rho-kinase pathway is therefore indispensable for smooth muscle contraction. GGPP is one of the downstream components of the mevalonate pathway and plays an important part in the Rho/Rho-kinase pathway activation. Thus, statins, which regulate the mevalonate pathway, also regulate the Rho/Rho-kinase pathway and, consequently, MLC phosphorylation.

Previously, we reported that the Rho-kinase pathway is involved in TGF-β2–induced MLC phosphorylation and contraction of hyalocyte-containing collagen gels and that hydroxyfasudil, a potent Rho-kinase inhibitor, significantly diminishes these TGF-β2–induced effects (18). In the present study, we investigate the regulatory effects of statins on TGF-β2– and vitreous-dependent MLC phosphorylation and contraction of hyalocyte-containing collagen gels and their therapeutic potential for prevention of PVDs in vivo.

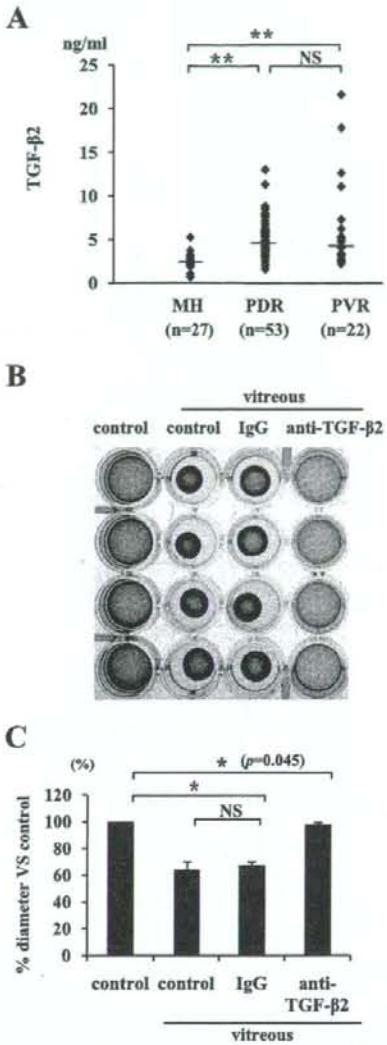

FIG. 1. TGF-β2 expression in the vitreous. *A*: Vitreous samples were collected from patients with non-PVD (macular hole) and PVD (PDR and PVR). Concentrations of TGF-β2 in the vitreous were measured by enzyme-linked immunosorbent assay (macular hole, $n = 27$; PDR, $n = 53$; PVR, $n = 22$). **$P < 0.01$ compared with macular hole. *B*: Hyalocytes were embedded in type I collagen gels ($n = 4$). After starvation and pretreatment with 1 μg/ml anti–TGF-β2 antibody or 1 μg/ml IgG for 1 h, the collagen gels were treated with vitreous samples from patients with PVD. Five days after the treatment, the gels were photographed. *C*: The diameter of the collagen gels was measured and expressed as percentage of the average diameter of the control group. *$P < 0.05$.

RESEARCH DESIGN AND METHODS

Reagents. Simvastatin, fluvastatin, pravastatin, and cerivastatin were purchased from CalBiochem (La Jolla, CA). Lovastatin was purchased from Funakoshi (Tokyo). Simvastatin was used as an active form after treatment with NaOH.

Vitreous samples and enzyme-linked immunosorbent assay. This study was carried out with approval from the Institutional Review Board and performed in accordance with the ethical standards of the 1989 Declaration of Helsinki. We obtained written informed consent from the patients. Vitreous samples were collected from patients who underwent pars plana vitrectomy because of non-PVD (macular hole) or PVD (PDR and PVR). Concentrations of TGF-β2 were measured by a human TGF-β2 immunoassay kit (R&D Systems, Minneapolis, MN).

Cell culture. Bovine hyalocytes were isolated as we previously reported (33). Cultured hyalocytes obtained between passages 5 and 7 were used in experiments.

Collagen gel contraction assay. The contraction assay was performed as we previously described (33). Type I collagen (Koken, Tokyo), a reconstitution buffer, hyalocytes suspension, and distilled water were mixed and added to a 24-multiwell plate (Nunc, Roskilde, Denmark). After 1-h pretreatment of vitreous samples with 1 μg/ml anti–TGF-β2 antibody (R&D Systems) or 1 μg/ml mouse IgG (Sigma-Aldrich) that was added for confirming the absence of nonspecific suppression of the gel contraction by anti–TGF-β2 antibody, the gels were treated with the vitreous samples (400 μl). The diameter of the collagen gel was measured at 5 days after the treatment. For quantitative purposes, contraction data are presented as the reduction in diameter of the collagen gels.

In the same way, collagen gels containing hyalocytes were starved, pretreated with statins for 24 h, and then treated with 3 ng/ml TGF-β2 (Sigma-Aldrich) or vitreous samples.

Western blot analysis. Total cell lysates were subjected to 15% SDS-PAGE, and the blots were incubated with an antibody against phosphorylated-MLC (*p*-MLC; 1:1,000; Santa Cruz Biotechnology, Santa Cruz, CA). Visualization was performed with an enhanced chemiluminesence (ECL; Amersham, Arlington